ELSEVIER

Journal of Electron Spectroscopy and Related Phenomena 82 (1996) 23–29

JOURNAL OF ELECTRON SPECTROSCOPY and Related Phenomena

Wavenumber dependence of the energy loss function of graphite and aluminium

Domingo J. Planes[a], Rafael Garcia-Molina[a,*], Isabel Abril[b], Néstor R. Arista[c]

[a]*Departamento de Física, Universidad de Murcia, Apdo. 4021, E-30080 Murcia, Spain*
[b]*Departament de Física, Universitat d'Alacant, Apt. 99, E-03080 Alacant, Spain*
[c]*Centro Atómico Bariloche, Instituto Balseiro, RA-8400 Bariloche, Argentina*

Received 20 July 1995; accepted 12 February 1996

Abstract

The energy loss function of a material is a key parameter in the dielectric formalism used to describe the optical spectra and the excitations produced by swift charges in solids. Modelling the experimental energy loss function as a sum of Mermin type functions in the optical limit (i.e., at zero momentum transfer), we have calculated its dependence on the momentum transfer. We compare the result with available experimental data for graphite and aluminium and with other theoretical models. We find a reasonably good agreement of our results with these data, and better agreement than is obtained with other models.

Keywords: Dielectric function; Electron energy loss spectroscopy; Energy loss function

1. Introduction

In studies related to the transport of electrons in solids, it is interesting to describe with sufficient accuracy the spectra of the transfer of both momentum and energy to the target electrons. The dielectric treatment to describe the response of the target to external probes has successfully been applied in quantitative chemical analysis [1], reflection electron energy loss spectroscopy [2] and Monte Carlo simulations of electron scattering in solids [3]. In all these cases the energy loss function (ELF) plays a key role, because it contains the response of the material to the external perturbations. The ELF of a system may be obtained experimentally by sending photons or electrons to the material and analysing the corresponding spectra.

A useful scheme to describe the response of the target electrons to external perturbations is provided by the random phase approximation for calculating the dielectric function of an electron gas, a procedure that was first developed by Lindhard [4]; however, the Lindhard dielectric function predicts an infinite life for plasmons, whereas it is well known that in real materials these excitations are damped. Although it seems to be a straightforward substitution, the replacement of ω by $\omega+i\gamma$ in the Lindhard dielectric function, where γ represents the plasmon damping, is erroneous, as it does not conserve the local particle number. Mermin [5] derived an expression for the dielectric function that took into account the finite lifetime of the plasmons and also preserved the local particle number; however, presumably because of its algebraic complexity, there seems to be a lack of applications of this function. In the present paper we use this formulation to calculate the ELF of a material,

* Corresponding author.

PII S0368-2048(96)03043-5

specifically to describe its wavenumber dependence, which compares better than other models with available experimental data. The Appendix contains a brief summary of the mathematical expressions needed to handle Lindhard's and Mermin's dielectric functions $\epsilon_L(q,\omega)$ and $\epsilon_M(q,\omega)$, respectively.

Various models have been proposed to describe the response of the target electrons to excitations produced by an external probe, such as a swift electron. One of the most widely employed models uses the dielectric formalism, in which the main input magnitude is the ELF; once the ELF is known, it is relatively easy to calculate other energy loss related quantities (e.g., the inverse mean free path, stopping power, energy loss straggling, etc.). However, to carry out this procedure properly it is necessary to know the wavenumber dependence (the wavevector for anisotropic materials) of the target excitations.

In Section 2 we propose an extension of the ELF to non-zero values of the wavenumber that is based on a representation of the experimentally determined optical ELF as a sum of Mermin type [5] ELFs. In Section 3 we apply this procedure to graphite and aluminium, obtaining a fairly good agreement with the known energy loss and wavenumber dependent ELF for both materials. Finally, in Section 4 we discuss the quality of our results as compared with experimental data and other models.

2. Model

The dielectric formalism for studying the interaction of a swift charged particle with matter was initially introduced by Fermi [6] and successfully developed by other authors [7–10]. It is commonly accepted that this formalism provides a useful approach to the evaluation of the magnitudes related to the transfer of energy and momentum from the projectile to the target electrons. In this framework, the key property used to describe the response of the medium to an external perturbation is the dielectric function $\epsilon(q,\omega)$, where $\hbar\omega$ and $\hbar q$ are the energy and the momentum transferred to the target electrons in an inelastic event. When we consider a homogeneous and isotropic system the dielectric function is a scalar (instead of a tensor) quantity and depends only on the magnitude of the wavevector, i.e, the wavenumber q, but not on its direction $\epsilon(q,\omega)$. From the dielectric function it is possible to obtain the energy loss function $\mathrm{ELF}=\mathrm{Im}[-1/\epsilon(q,\omega)]$, which is the basic input quantity in all the magnitudes related to the stopping theory. This function determines the probability that an inelastic event with momentum transfer $\hbar q$ and energy transfer $\hbar\omega$ takes place in the target. Unfortunately the ELF is provided most of the time for zero wavenumber through optical experiments, and a large amount of data exists for these conditions [11–14].

During the last few years several schemes to extend the ELF, as evaluated from optical ($q=0$) data, to the non-zero momentum transfer region ($q\neq 0$) have been proposed. For instance, Tanuma et al. [15] developed an earlier model by Penn [16] using experimental optical data to describe the dependence on the energy loss and the Lindhard dielectric function to represent the dependence on momentum transfer. Also, Ashley et al. [17] introduced a model based on fitting of the optical ELF by means of a Drude type ELF and an analytical extension to the momentum space.

In this work we suggest the use of the Mermin [5] dielectric function ϵ_M to construct the ELF of a material, because this function allows one correctly to incorporate the electron collision time. This avoids the mathematical problem of extending the ELF to the q-space, as this is automatically provided by the analytical dependence of $\epsilon_M(q,\omega)$. We proceed by fitting the experimental ELF of a material at $q=0$ by a sum of the Mermin type ELF, viz.

$$\mathrm{Im}\left[\frac{-1}{\epsilon(q=0,\omega)}\right]_{\mathrm{experimental}} = \sum_i A_i \mathrm{Im}\left[\frac{-1}{\epsilon_M(\omega_i,\gamma_i;q=0,\omega)}\right] \tag{1}$$

where ω_i and γ_i are related to the position and width of each peak in the energy loss spectrum. The coefficients A_i are determined under the requirement that the sum rule

$$N_{\mathrm{eff}}(\omega) = \frac{m}{2\pi^2 e^2 n}\int_0^{\omega} \mathrm{d}\omega'\omega' \mathrm{Im}\left[\frac{-1}{\epsilon(q,\omega')}\right] \tag{2}$$

must be satisfied. In the above Eq. (2), m and e represent the electronic mass and charge, respectively, and n represents the atomic density. This sum rule provides the effective number of electrons per target atom $N_{\mathrm{eff}}(\omega)$ which participate in the target

Table 1
Parameters used to fit the ELF of graphite and aluminium through Eq. (1)

i	Graphite			Aluminium		
	A_i	$\hbar\omega_i$/eV	$\hbar\gamma_i$/eV	A_i	$\hbar\omega_i$/eV	$\hbar\gamma_i$/eV
1	0.0277	0.136	1.142	1.1178	14.987	0.952
2	0.1847	6.99	1.768			
3	0.1309	19.31	6.80			
4	0.6187	27.88	5.44			
5	0.0713	38.08	68.0			

excitations up to an energy $\hbar\omega$. As $\hbar\omega \to \infty$, N_{eff} should tend to the total number of electrons per atom, a sum rule that must be satisfied independently of the value of the momentum transfer.

The graphite ELF at $q=0$ has been taken from electron energy loss experiments [18], and it shows a structure with two main peaks, one at low energy, ~7 eV, and another at ~27 eV. The first peak is related to a plasmon due to the π electrons, and the second peak concerns a plasmon due to the π and σ electrons. The aluminium ELF at $q=0$ was taken from Ref. [11], and it clearly shows only a prominent peak at 15 eV. The values of the parameters used in Eq. (1) to fit the ELF of graphite and aluminium are given in Table 1.

The effective number of electrons as a function of the energy transfer is depicted in Fig. 1(a) and 1(b) for graphite and for aluminium, respectively. We can clearly observe that, if inner shell electrons are not considered, the effective numbers agree with the number of valence electrons: four for graphite and three for aluminium. As q increases, the plateaux in the curves shift to larger values of ω, owing to a redistribution of the oscillator strengths for $q \neq 0$. As the experimental $q=0$ – ELF are usually available for $\hbar\omega \leq 50$ eV, the effects of inner shells in the energy loss spectra have been taken into account by properly converting to ELF the available atomic scattering factors [19]. The inner shell electrons appear at $E_K = 284$ eV for graphite and $E_L = 72.5$ eV for aluminium [20], which coincide, when $q=0$, with the abrupt change in the plateaux of N_{eff} depicted in Fig. 1.

Other models [2,17] for the ELF also use a fitting to the experimental (optical) ELF, complemented with a suitable algorithm to extend it to the non-zero momentum transfer region, of the form $\text{Im}[-1/\epsilon(q,\omega)] = \text{Im}[-1/\epsilon(q=0,\omega(q))]$, providing different expressions for $\omega(q)$. In particular, we compare our calculations with the model introduced by Ashley et al. [17], hereafter referred to as the extended Drude model, in which

$$\text{Im}\left[\frac{-1}{\epsilon(q,\omega)}\right] = \sum_i B_i \frac{\gamma_i \omega}{[\omega^2(q)-\omega^2]^2+\gamma_i^2\omega^2} \tag{3}$$

where $\omega(q) = \omega_i + \hbar q^2/2m$ and now the coefficients B_i should be chosen to satisfy the sum rule given by eqn (2). It is worth noting that both models, Eq. (1) and Eq. (3), coincide at $q=0$. In fact, at $q=0$ they correspond to the ELF given by the Drude model where, for each set of parameters (ω_i,γ_i),

$$\text{Im}\left[\frac{-1}{\epsilon(q=0,\omega)}\right] = \frac{\gamma_i \omega}{(\omega_i^2-\omega^2)^2+\gamma_i^2\omega^2} \tag{4}$$

Then the parameters A_i in Eq. (1) and B_i in Eq. (3) represent the relative strength of each resonance in the ELF as described by the respective model, Eq. (1) or Eq. (3), respectively.

In spite of their coincidence at $q=0$, as q increases the differences between the two models will become more significant, as will be seen in Section 3.

3. Results

In Fig. 2 and Fig. 3 we show the behaviour of the ELF in the available experimental range: the region of (0–1) Å^{-1} transferred momentum and 0–40 eV energy loss for graphite [21], and the region of (0–3) Å^{-1} and 0–100 eV for aluminium [22], respectively. The graphite ELF was obtained [21] through electron energy loss measurements with 60 keV electrons in ≈ 1000 Å thick crystalline samples, providing the ELF for q oriented perpendicularly to the optical axis in two non-equivalent directions, but there were minor differences in the corresponding ELFs and we have

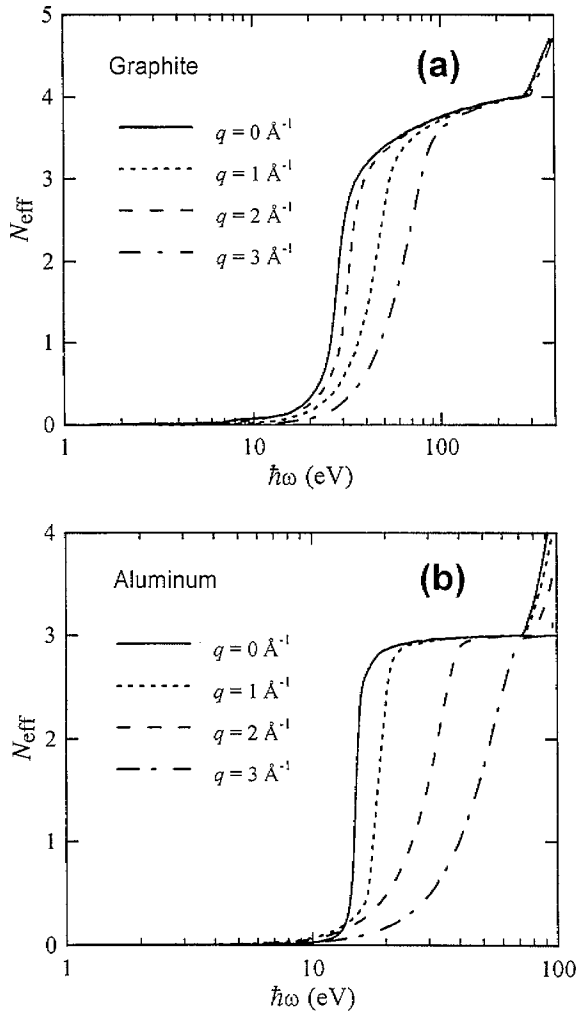

Fig. 1. Effective number of electrons participating in excitations with energy transfer $\hbar\omega$ and momentum transfer $\hbar q$: (a) graphite, (b) aluminium.

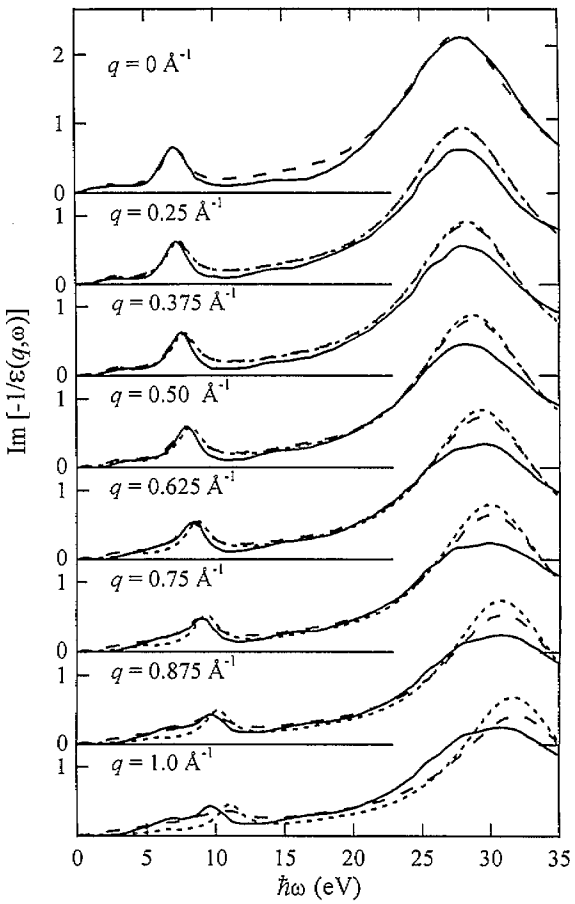

Fig. 2. Graphite energy loss function versus the energy transfer $\hbar\omega$, plotted at different values of the momentum transfer $\hbar q$: experimental results [21] (full line), present calculations (long dashed line), and extended Drude model [17] (short dashed line).

used an average of the ELF from the two directions. The ELF data for aluminium were obtained [22] from intensity measurements for the inelastic scattering of 75 keV electrons through ≈ 1000 Å thick polycrystalline foils.

Both models, the one presented in this paper and the extended Drude model [17], coincide at $q = 0$, but they differ in the manner in which the extension to the $q \neq 0$ region is made. Although both models give similar values of the ELF for small q ($\neq 0$) and both agree reasonably well with the corresponding experimental data, we can see that for large values of q the model using a sum of Mermin type ELFs more closely follows the experimental data. The differences between the two models are especially sizeable for the case of aluminium (Fig. 3). The broadening of the ELF peaks is better reproduced with the present treatment, as can be seen through the evolution of the low energy peak in the case of graphite and that of the main peak in the case of aluminium. It is worth mentioning that the small peak appearing in the aluminium ELF at $q = 1$ Å^{-1} corresponds to the excitation of a double plasmon

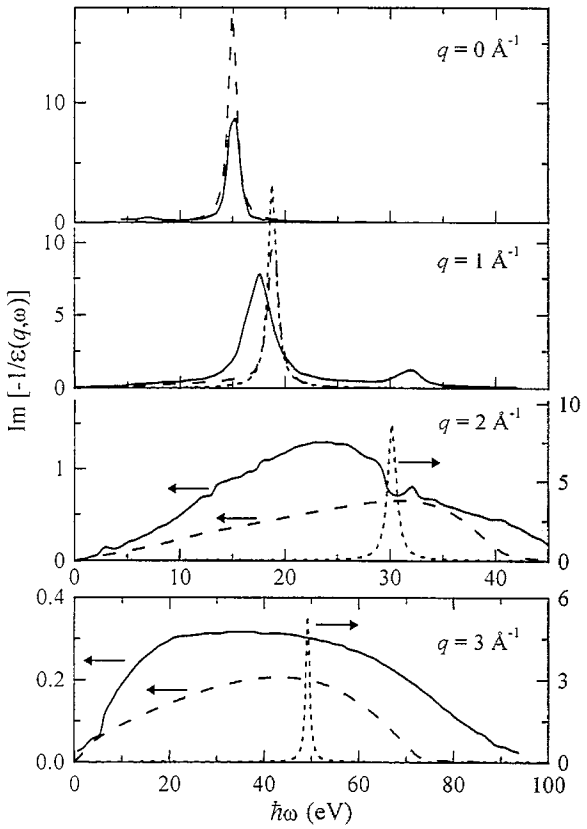

Fig. 3. Aluminium energy loss function versus the energy transfer $\hbar\omega$, plotted at different values of the momentum transfer $\hbar q$: experimental results [22] (full line), present calculations (long dashed line), and extended Drude model [17] (short dashed line).

[22], and that for large momentum transfer the experimental data contain significant statistical uncertainties [22]; however, the general trends in the ELF curves are reproduced better by our results than with the extended Drude model [17], in which the peak keeps its sharp shape (with minor changes) as q increases, in contrast to the observed experimental behaviour.

This gradual loss of the initial structure in the ELF is well understood, as the plasmon (responsible for the peaks in the ELF) must decay into individual excitations at some critical wavenumber q_c, when the plasmon curve enters the individual excitations region in the dispersion relationship; the value of q_c is obtained numerically and corresponds to the intersection of the implicit curve $\epsilon_L(q,\omega)=0$, which gives the plasmon line corresponding to Lindhard's dielectric function $\epsilon_L(q,\omega)$ and the explicit function $\hbar\omega=\hbar^2(q^2+2qq_F)/2m$, which limits by the left the individual excitations region (q_F is the Fermi wavenumber of the material).

For graphite there are two plasmon peaks, one at ≈ 7 eV and the other at ≈ 27 eV; we have calculated the corresponding values for q_c to be ≈ 0.9 Å^{-1} and ≈ 1.6 Å^{-1}, respectively. In Fig. 2 we can appreciate how the ≈ 7 eV peak almost loses its shape at $q \approx 1$ Å^{-1}, in good agreement with our calculation; unfortunately there are no available data for $q > 1$ Å^{-1} from which to check how the ≈ 27 eV peak behaves when $q \approx 1.6$ Å^{-1}. For aluminium, we find that the plasmon peak at 15 eV merges into the individual excitations region at $q_c = 1.3$ Å^{-1}, in excellent agreement with the experimental value [23].

The plasmon peaks in the ELF then lose prominence as q increases, as in the limit $q \to \infty$ no collective behaviour should be observed. At large wavenumber, single excitations predominate over the collective effects, this being related to the loss of structure in the ELF.

Let us point out here that there are also ab initio treatments [24–26], where a detailed description of the target (band structure, charge exchange, etc.) can successfully be applied to only a reduced number of systems. These serve as a check and a guide to compare with the results of less sophisticated but easier to use models, like the one discussed in this paper. The results reported by Lee and Chang [25] for the ELF of aluminium along a given direction in the momentum space compare well with our calculations; however, their peak height differs considerably from our result and the experimental values [22].

It is worth noting that the wavenumber evolution of the Ashley et al. ELF retains the initial structure in the ELF even at high momentum transfer values, although displaced to higher energies.

4. Summary and conclusions

In the interaction of radiation with matter the ELF plays a key role, because it contains the response of the material to external perturbations. Introducing the q dependence of the ELF through the Mermin dielectric function provides a natural extension of the

wavenumber dependence of the ELF, giving results that agree better with the experimental ELF than those of other models introduced previously [17]. Furthermore, it compares fairly well with energy integrated quantities, such as the stopping power, even at low energies [27]. An advantage of this treatment is that it can be applied to both conductors and insulators, the only input data being the ELF at zero momentum transfer, a magnitude available as optical data for many materials [11–14].

Although several methods have been proposed to extend the energy loss function at $q=0$ to the region with $q \neq 0$, and most of them provide a satisfactory basis for the calculation of such integrated quantities as the stopping power or the energy loss straggling, they fail to reproduce correctly the energy loss spectra. This is so because the stopping power and the straggling (which are integrated magnitudes) are not very sensitive to the details of the ELF, provided that some constraints (e.g. sum rules and plasmon peak location) are satisfied.

Acknowledgements

We thank the Spanish DGICYT (Projects PB92-0341 and PB93-1125) for financial support. N.R.A acknowledges the support of the Generalitat Valenciana through the Programa PROPIO.

Appendix A

This appendix contains the main expressions concerning Lindhard's and Mermin's dielectric functions, $\epsilon_L(q,\omega)$ and $\epsilon_M(q,\omega)$ respectively. The Mermin dielectric function $\epsilon_M(q,\omega)$ describes an electron gas in the relaxation time approximation and conserves the local number of electrons. The analytical form of this complex dielectric function is given by [5]

$$\epsilon_M(q,\omega)=1+\frac{(1+i\gamma/\omega)[\epsilon_L(q,\omega+i\gamma)-1]}{1+(i\gamma/\omega)[\epsilon_L(q,\omega+i\gamma)-1]/[\epsilon_L(q,0)-1]} \tag{A1}$$

Here, γ is related to the damping of the excitations in the electron gas, which gives a finite lifetime for the plasma oscillations and takes into account the effect of the dissipative processes that occur in real solids. For a degenerate free electron gas, Lindhard's dielectric function is given by [4]

$$\epsilon_L(q,\omega)=1+\frac{e^2}{\pi\hbar v_F z^2}[f_1(u,z)+if_2(u,z)] \tag{A2}$$

Here we have followed the usual nomenclature, writing ϵ_L as a function of the dimensionless variables $u=\omega/(qv_F)$ and $z=q/(2q_F)$, where v_F and q_F are the Fermi velocity and wavenumber, respectively. The dimensionless functions f_1 and f_2 are given by

$$f_1(u,z)=\frac{1}{2}+\frac{1}{8z}[g(z-u)+g(z+u)] \tag{A3}$$

and

$$f_2(u,z)=\begin{cases}\dfrac{\pi}{2}u, & \text{when } z+u<1\\ \dfrac{\pi}{8z}[1-(z-u)^2], & \text{when } |z-u|<1<z+u\\ 0, & \text{when } |z-u|>1\end{cases} \tag{A4}$$

where

$$g(x)=(1-x^2)\ln\frac{x+1}{x-1} \tag{A5}$$

References

[1] D.R. Penn, J. Electron Spectrosc. Relat. Phenom., 9 (1976) 29.
[2] F. Yubero, S. Tougaard, E. Elizalde and J.M. Sanz, Surf. Interface Anal., 20 (1993) 719.
[3] J.M. Fernández-Varea, R. Mayol, F. Salvat and D. Liljequist, J. Phys. Condensed Matter, 4 (1992) 2879; J.D. Martínez, R. Mayol and F. Salvat, J. Appl. Phys., 67 (1990) 2955.
[4] J. Lindhard, Mat. Fys. Medd. - K. Dan. Vidensk. Selsk., 28 (8) (1954).
[5] N.D. Mermin, Phys. Rev. B, 1 (1970) 2362.
[6] E. Fermi, Z. Phys., 29 (1924) 315.
[7] E. Fermi, Phys. Rev., 57 (1940) 485.
[8] J. Hubbard, Proc. Phys. Soc. London, Sect. A, 68 (1955) 976.
[9] J. Neufeld and R.H. Ritchie, Phys. Rev., 98 (1955) 1632.
[10] P. Nozières and D. Pines, Phys. Rev., 113 (1959) 1254.
[11] H.-J. Hagemann, E. Gudat and C. Kunz, Optical constants from the far infrared to the X-ray region: Mg, Al, Cu, Ag, Au, Bi, C, and Al_2O_3, Deutsches Elektronen-Synchrotron

Report DESY SR-74/7, Hamburg, 1974, unpublished. J. Opt. Soc. Am., 65 (1975) 742.
[12] R.-P. Haelbich, M. Iwan and E.E. Koch, Optical properties of some insulators in the vacuum ultraviolet region, No. 8-1, Physics Data, Hamburg, 1977.
[13] J.H. Weaver, C. Krafka, D.W. Lynch and E.E. Koch, Optical properties of metals. I and II, Physics Data No. 18-1 and 18-2, Fachinformationszentrum Karlsruhe, 1981.
[14] E.D. Palik (Ed.), Handbook of Optical Constants of Solids, Vols. I and II, Academic Press, Orlando, 1985, and Boston, 1991.
[15] S. Tanuma, C.J. Powell and D.R. Penn, Surf. Interface Anal., 11 (1988) 577; 17 (1991) 911; 17 (1991) 927; 20 (1993) 77; 21 (1994) 165.
[16] D.R. Penn, Phys. Rev. B, 35 (1987) 482.
[17] J.C. Ashley, J.J. Cowan, R.H. Ritchie, V.E. Anderson and J. Hoelzl, Thin Solid Films, 60 (1979) 361.
[18] H. Venghaus, Phys. Status Solidi B, 71 (1975) 609.
[19] B.L. Henke, P. Lee, T.J. Tanaka, R.L. Shimabukuro and B.K. Fujikawa, At. Data Nucl. Data Tables, 27 (1982) 1.
[20] D.R. Lide (Ed.), CRC Handbook of Chemistry and Physics, 73rd edn., CRC Press, Boca Raton, 1992.
[21] U. Büchner, Phys. Status Solidi B, 81 (1977) 227.
[22] P.E. Batson and J. Silcox, Phys. Rev. B, 27 (1983) 5224. Corrections to erroneous axis scales in Fig. 13 were kindly provided by the authors.
[23] The caption of Fig. 1 in Ref. [22] gives $q_c = 1.3\ \text{Å}^{-1}$ for aluminium.
[24] J.P. Walter and M.L. Cohen, Phys. Rev. B, 5 (1972) 3101.
[25] K.-H. Lee and K.J. Chang, Phys. Rev. B, 49 (1994) 2362.
[26] F. Aryasetiawan and K. Karlsson, Phys. Rev. Lett., 73 (1994) 1679.
[27] I. Abril, R. Garcia-Molina and N.R. Arista, Nucl. Instrum. Methods Sect. B, 90 (1994) 72.